ChemComm

A triplex-forming linear probe for sequence-specific detection of duplex DNA with high sensitivity and affinity

Journal:	*ChemComm*
Manuscript ID	CC-COM-03-2020-001865.R1
Article Type:	Communication

COMMUNICATION

A triplex-forming linear probe for sequence-specific detection of duplex DNA with high sensitivity and affinity

Yanglingzhi Chen,[a] Keiji Murayama,[a] Hiromu Kashida,[a] Yukiko Kamiya,[a] and Hiroyuki Asanuma*[a]

Received 00th January 20xx,
Accepted 00th January 20xx

DOI: 10.1039/x0xx00000x

A triplex-forming oligonucleotide (TFO) linear probe containing perylene derivatives was synthesized. The TFO linear probe formed a remarkably stable triplex with a target DNA duplex, resulting in light-up of fluorescence emission. The sensitivity was extremely high sensitivity even at pH 7. Detection of PCR-amplified target DNA was demonstrated.

Sequence-specific detection of DNA is important in wide range of applications including infectious disease diagnosis,[1-3] forensic analysis, [4] food safety evaluation, [5,6] and environmental monitoring.[7] Most strategies for detection of DNA depend on denaturation of double-stranded DNA (dsDNA) into single strands. Although the real-time PCR is an effective method for detection of dsDNA, it requires an expensive device that cannot be operated outside a laboratory.[8] Detection using an intercalating dye can result in false-positive signals in the absence of the target sequence.

Triplex-forming oligonucleotides (TFOs) bind in a sequence-specific manner to the major groove of dsDNA should be an effective detection method for dsDNA.[9-14] However, the TFO-based approach for sequence-specific DNA detection has relatively low sensitivity due to background emission, low thermal stability of Hoogsteen base pairs, [15,16] and a long response time for probes with hairpin structures.[17] To solve these problems, various strategies have been suggested.[18-21]

Previously, we reported validation of a type of linear probe for sequence-specific recognition of mRNA. These probes have multiple fluorophores tethered on acyclic D-threoninol and have extremely high signal-to-background (S/B) ratios and are able to detect mRNA both *in vitro* and *in situ*.[22,23] We reasoned that this strategy would be applicable for detection of dsDNA through triplex formation. The principle of this probe is schematically illustrated in Fig. 1. In the single-stranded state, the flexible linear probe causes hydrophobic interactions among the perylenes, lead to self-quenching. When it specifically hybridizes to complementary dsDNA forming a triplex structure, the fluorophores intercalate between nucleobases resulting in a fluorescence signal. The previously reported linear probe targeting single strand, could not directly detect dsDNA, whereas the TFO linear probe can bind to dsDNA with a fluorescence increasing response.

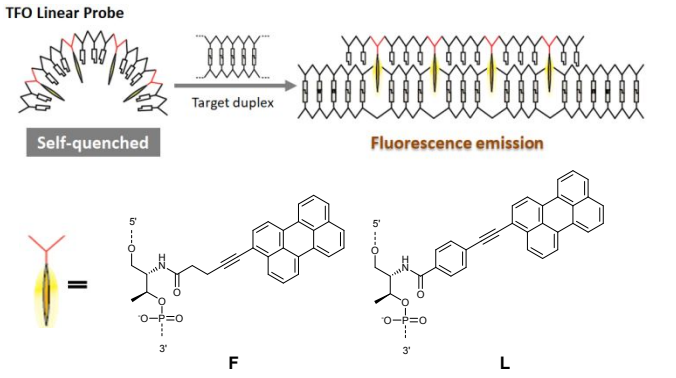

Figure 1. Illustration of TFO linear probe and chemical structures of perylene derivatives **F** and **L**.

A duplex formed from a strand with a poly-adenosine region (DNA-A) and a strand with a poly-thymidine region (DNA-T) was selected as a model target (Table 1). We designed TFO linear probes containing perylene residues (**F**) consisting of perylene linked to D-threoninol through a 1-butyne linker (Fig. 1).[24] To evaluate the effect of the number of fluorophores, we synthesized probes with no and with one, two, three, and four perylene residues (**0F-T**, **1F-T**, **2F-T**, **3F-T**, and **4F-T**, respectively) were synthesized. Based on data from our previous studies,[22,23] we incorporated **F** in three base-pair intervals.

Firstly, we evaluated thermal stability of the triplexes formed between the target duplex and each probe by measuring UV-

[a] *Graduate School of Engineering, Nagoya University, Furo-cho, Chikusa-ku, Nagoya 464-8603 (Japan)*
E-mail: asanuma@chembio.nagoya-u.ac.jp

Electronic Supplementary Information (ESI) available: [details of any supplementary information available should be included here]. See DOI: 10.1039/x0xx00000x

Table 1. Sequences of target DNA duplex and TFO linear probes[a]

Target dsDNA	**DNA-A**	5'-CGTCGGTTT-A_{13}-TTTCGTGGC-3'
	DNA-T	3'-GCAGCCAAA-T_{13}-AAAGCACCG-5'
Probes	**0F-T**	5'-TTTTTTTTTTTTT-3'
	1F-T	5'-**F**TTTTTTTTTTTT-3'
	2F-T	5'-**F**TTT**F**TTTTTTTTTT-3'
	3F-T	5'-**F**TTT**F**TTT**F**TTTTTTT-3'
	4F-T	5'-**F**TTT**F**TTT**F**TTT**F**TTTT-3'
	3L-T	5'-**L**TTT**L**TTT**L**TTTTTT-3'

a. **F**: F-type perylene, **L**: L-type perylene

melting and fluorescence-melting curves.[25] The native DNA strand (**0F-T**) formed a triplex in buffer containing 1.0 M Mg^{2+}; however, no triplex was formed (T_m < 10 °C) when the Mg^{2+} concentration was 10 mM or 100 mM (Fig. 2a, Fig. S1, Table S1). T_m values for triplexes increased with the number of **F** residues. For example, the T_m of **3F-T** was 42.6 °C in 10 mM Mg^{2+}, whereas that of **1F-T** was 17.4 °C. Triplex stabilization is likely due to the strong stacking interaction of **F** residues within the triplex.

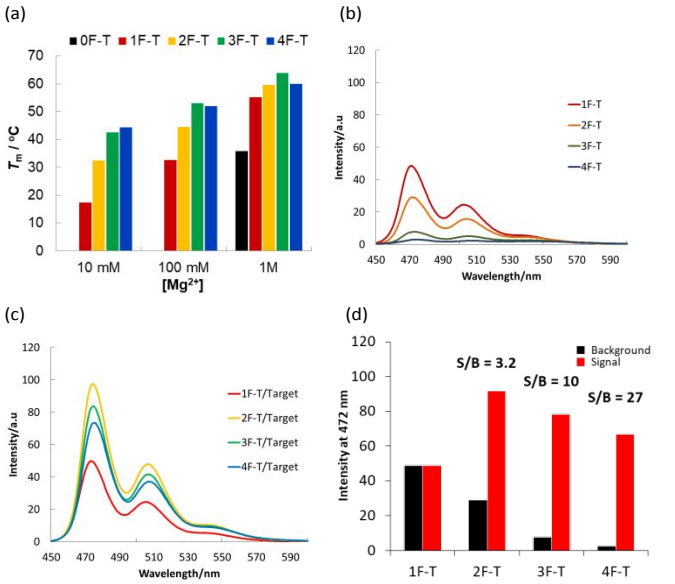

Figure 2. (a) Comparison of melting temperatures of the triplexes at indicated concentrations of Mg^{2+}. Conditions: 1.0 μM linear probe and DNA-A, 1.1 μM DNA-T, 90 mM TBM buffer (90 mM Tris borate,pH 7.0 with indicated concentration of $MgCl_2$). (b and c) Fluorescence spectra of (b) single strand probes and (c) triplexes formed with **1F-T** (red lines), **2F-T** (yellow lines), **3F-T** (green lines), and **4F-T** (blue lines). Conditions: ex. = 440 nm, 1.0 μM linear probe and DNA-A, 1.1 μM DNA-T, 90 mM TBM buffer ($MgCl_2$=100 mM), 20 °C. (d) Fluorescence intensity at 472 nm and S/B ratios. Conditions: ex. = 440 nm, 1.0 μM linear probe and DNA-A, 1.1 μM DNA-T, 90 mM TBM buffer ($MgCl_2$=100 mM), pH 7.0, 20 °C.

Next, we investigated fluorescence spectra of these probes (Fig. 2b-d). Absorption spectra were also measured (Fig. S2). In the single-stranded state, intensity was reduced as the number of **F** residues increased, due to the self-quenching effect. In contrast, the emission intensity increased with the number of **F** residues in the context of a triplex, because fluorophores were separated by the base pairs. As a result, the S/B ratio was higher for probes with more fluorophores (Fig. 2d). Simultaneously, a slight reduction of the signal emission was observed for **3F-T** and **4F-T** compared with **2F-T**. Consequently, a probe with three fluorophores (**3F-T**) was optimal: This probe hybridized with target dsDNA with the highest affinity and a high S/B ratio of 10.

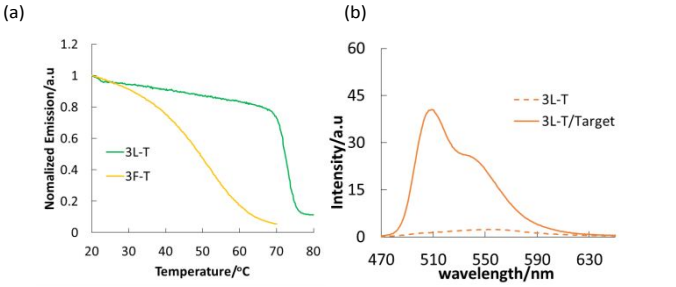

Figure 3. (a) Fluorescent-melting curves of **3F-T** (yellow line) and **3L-T** (green line) at 100 mM [Mg^{2+}]. (b) Fluorescence spectra in the absence (dashed line) and presence (solid line) of target dsDNA. Conditions: for F type perylene ex. = 440 nm; for **L** type perylene, ex. = 455 nm; 1.0 μM linear probe and DNA-A, 1.1 μM DNA-T, 90 mM TBM buffer ($MgCl_2$=100 mM), pH 7.0, 20 °C.

To increase the affinity of the probe for a DNA duplex, we re-considered the structure of fluorophore. Molecular modelling revealed that the **F** residue was smaller than the triple-base-pairing plane (Fig. S3). We hypothesized that a larger conjugation system would enhance stacking and would stabilize the triplex form. We therefore prepared **3L-T** containing three **L**-perylenes (Fig. 1); this perylene derivative has an expanded conjugation system relative to **F**-perylene.[24] Interestingly, the triplex formed with **3L-T** had a higher thermal stability than that formed with **3F-T** (Fig. 3a, S1 and Table S1). The **3L-T** triplex had a T_m of 72.7 °C at 100 mM Mg^{2+}, whereas that of the **3F-T** triplex under the same conditions was 53.1 °C. The S/B ratio of **3L-T** was 28 (Fig. 3b), which was comparable to the S/B ratio of **4F-T**. Notably, the **L** residue interferes with duplex formation.[24] Hence, incorporation of the **L**-perylenes suppresses undesirable duplex formation between DNA and the probe (Fig. S4), which is an advantage of use of **L**-type perylene.

Table 2. Sequences of AR duplex strands and TFO linear probes[a]

Target dsDNA2	**AR-as**	5'-CTACT-AAAGAAGAAAAGAGAGAAG-AATC-3'
	AR-s	3'-GATGA-TTTCTTCTTTTCTCTCTTC-TTAG-5'
Probes	**0L-X**	5'-TTTCTTCTTTTCTCTCTT-3'
	3L-X	5'-**L**TTT**L**CTT**L**CTTTTCTCTCTT-3'
	3L1gQ	5'-**L**TTT**L**CTT**L**CTTTTC**gQ**TCTCTT-3'

a. **as**: antisense, **s**: sense, **gQ**: gQ type anthraquinone

Next, we chose to evaluate probes targeting a region of the gene encoding the human androgen receptor (AR), a protein targeted for prostate cancer treatment.[26,27] This sequence selected contains cytosine that requires acidic condition for the G-C+ Hoogsteen pair formation,[15,16] which is an obstacle in the detection of this gene using a TFO probe. We hypothesized that high affinity of the TFO linear probe containing perylene might overcome this pH dependency. The TFO linear probe **3L-X** targeting the *AR* sequence was compared with **0L-X** (Table 2). At pH 7.0, the T_m of the triplex

formed with **0L-X** was 40.0 °C. The triplex formed with **3L-X** had a considerably higher T_m of 62.7 °C (Fig. 4a and Fig. S5). Light-up was observed with the **L**-perylene-containing probe **3L-X** upon triplex formation, and the S/B ratio was 14.7 (Fig. 4b).

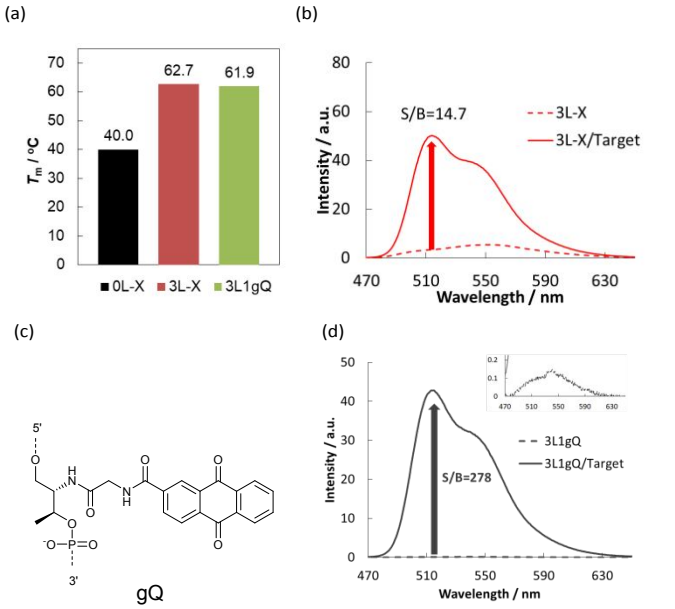

Figure 4. (a) Melting temperatures of triplexes formed between target dsDNA2 and **0L-X**, **3L-X**, and **3L1gQ**. (b) Fluorescence spectra of **3L-X** in the absence (dashed line) and presence (solid line) of target dsDNA2. (c) Chemical structure of **gQ**. (d) Fluorescence spectra of **3L1gQ** in the absence (dashed line) and presence (solid line) of target dsDNA2. Conditions: ex. = 455 nm; 1.0 μM linear probe and AR-as, 1.1 μM AR-s, 90 mM TBM buffer ($MgCl_2$=100 mM), pH 7.0, 20 °C.

Although **3L-X** successfully detected the target dsDNAs, background emission was observed from the single strand. To remove this emission, we incorporated an anthraquinone into the TFO linear probe as a quencher.[28] In order to ensure intercalation of the anthraquinone, a glycine linker was inserted between D-threoninol and anthraquinone (Fig. 4c).[29] This **gQ** residue was placed six residues away from the 3'-most **L** in **3L1gQ** to avoid the quenching in the triplex state (Table S2). The emission intensity of single-stranded **3L1gQ** was 0.15 and that of **3L1gQ**/dsDNA2 triplex was 41.7 (Fig. 4d, Fig. S6, and S7), for an S/B ratio of 278. Thus, a probe containing three **L**-perylenes and **gQ** formed a triplex with high thermal stability and excellent S/B at pH 7.0. Further stabilization of the triplex was observed at pH 5.5 (Fig. S15). The emission intensity of **3L1gQ** was significantly lowered in the presence of single-base mismatch target (1MM) and double-base mismatch target (2MM), compared to full-match target, proving its sequence-specificity and weak off-target effect (Figure S14, Table S4). Besides, **3L1gQ** could discriminate target dsDNA and complementary ssDNA: duplex of **3L1gQ**/**AR-as** showed lower T_m and smaller emission intensity than the triplex did (Fig. S17).

Finally, we evaluated sequence-specific detection of a PCR product. We constructed three plasmids as templates for PCR: plasmid 0 contained no target site, plasmid 2 contained two repeats of the *AR* gene sequence, and plasmid 5 contained five repeats (Fig. 5a, Fig. S8, and Table S3). Using **3L1gQ** as a probe during conventional real-time PCR resulted in successful detection of target dsDNA, and the amplification curve was comparable with the result obtained using SYBR Green I dye (Fig. S9).

We next mixed the PCR products after 30 thermal cycles with **3L1gQ** and glycerol (glycerol inhibits non-specific fluorescence) to evaluated fluorescence. Addition of **3L1gQ** resulted in strong fluorescence in the presence of the PCR products of plasmids 2 and 5, but plasmid 0 PCR products gave only a weak fluorescence (Fig. 5b). We also confirmed that PCR product of plasmid 1 containing only one *AR* gene sequence could also be detected by increasing in the fluorescence intensity (Fig. S13), demonstrating the detection of practical target containing single target place.

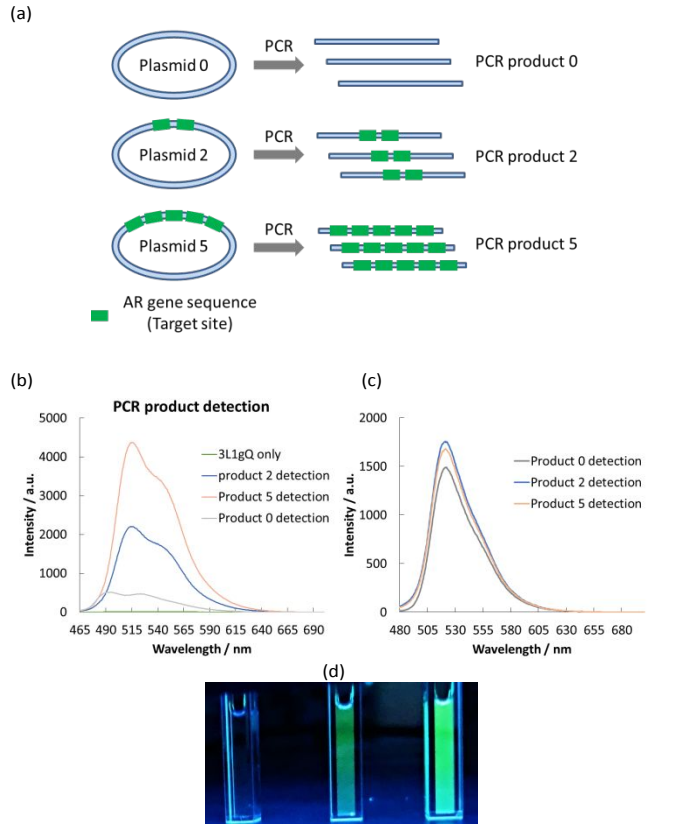

Figure 5. (a) Design of plasmids to yield PCR products with and without the *AR* target. (b) Direct fluorescence detection of dsDNA after PCR. Conditions: 1.0 μM **3L1gQ**, 50 μL crude PCR product, 9 vol% glycerol within 90 mM TBM buffer ($MgCl_2$=100 mM), pH 7.0 in a final volume of 200 μL, 20 °C. ex. = 455 nm. (c) Direct fluorescence detection using 0.025 vol% SYBR Green I (10,000X in DMSO), ex. = 470 nm. (d) Photograph of PCR products of plasmids 0, 2, and 5 in solution with **3L1gQ** excited using a hand-held UV-lamp (254 nm).

SYBR Green I showed fluorescence emission in the presence of target dsDNA (products of plasmids 2 and 5) and also in the presence of DNA without the target site (product of plasmid 0) (Fig. 5c). Thus, such conventional intercalator indiscriminately lighted-up dsDNA without the target site, while the linear probe showed the fluorescence only by responding to the target sequence. The S/B ratios in the presence of **3L1gQ** were 168 for the PCR product of plasmid 2 and 232 for the PCR

product of plasmid 5. These results confirm the sequence-specificity of the TFO linear probe.

The fluorescence of the linear probe was visible to the naked eye when target dsDNA was present (Fig. 5c), indicating that specialized equipment is not necessary for an assay involving this TFO probe. It should be noted that the no annealing step was required in the detection,[22] in contrast to the process used with probes that recognize single-stranded DNA. After addition of **3L1gQ** into PCR products, a clear signal emission immediately appeared (Fig. S10).

The crude PCR products after different numbers of cycles were evaluated by this method. As we expected, increasing the number of thermal cycles increased fluorescence intensity (Fig. S11), indicating that the TFO linear probe **3L1gQ** can be used to quantitate the target dsDNA.

To confirm the triplex formation between the TFO linear probe and dsDNA in PCR product, native PAGE was performed, and bands were visualized by inherent perylene fluorescence of **3L1gQ** and SYBR Gold staining (Fig. S12). As shown by SYBR Gold staining, the mobilities of the bands of PCR products of plasmids 2 and 5 were retarded in the presence of the probe, whereas the mobility of the product of plasmid 0 was the same in the presence and absence of **3L1gQ**. In addition, fluorescence from perylene was observed only in shifted bands. These results demonstrate that the probe sequence-specifically forms a triplex with the target DNA present in PCR products.

In conclusion, we have successfully developed a D-threoninol-based TFO linear probe that can specifically form a triplex with target dsDNA. The thermal stability of the triplexes increased with the number of perylenes in the probe. Use of **L**-perylene and anthraquinone enhanced stabilization relative to **F**-perylene and improved the S/B ratio. The optimal TFO linear probe had extremely high emission efficiency with an S/B ratio as 278 and high thermal stability (61.9 °C) at pH 7. In addition, quantitative detection of DNA after PCR was demonstrated. This type of probe could be used for direct detection of PCR products without need for specialized equipment; therefore, this type of TFO linear probe has potential for use in diagnostic testing.

Conflicts of interest

There are no conflicts to declare.

Acknowledgment

This work was supported by Japan Science and Technology Agency under Adaptable and Seamless Technology Transfer Program through Target-driven R&D (A-STEP) and AMED under Grant Number 19am0401007. Support from JSPS KAKENHI (grants JP18H03933 to H.A., JP16H05925 to H.K. and JP17K14514 to K.M.) and the Asahi Glass Foundation (to H.A.) are gratefully acknowledged.

Notes and references

1 B. A. Armitage, *Curr. Opin. Chem. Biol*. **2011**, *15*, 806–812.
2 H. J. Tanke, R. W. Dirks, T. Raap, *Curr. Opin. Biotechnol.* **2005**, *16*, 49–54.
3 J. Lederberg, N. York, *Microbiology* **1998**, *95*, 12637–12640.
4 M. A. Jobling, P. Gill, *Nat. Rev. Genet*. **2004**, *5*, 739–751.
5 Y. Wang, T. V. Duncan, *Curr. Opin. Biotechnol*. **2017**, *44*, 74–86.
6 C. A. Auer, *Trends Plant Sci.* **2003**, *8*, 591–597.
7 J. Wang, *Anal. Chim. Acta* **1997**, *347*, 1–8.
8 M.J. Espy, J.R. Uhl, L.M Sloan, S.P. Buckwalter, M.F. Jones, E.A. Vetter, J.D. Yao, N.L. Wengenack, J.E. Rosenblatt, F.R. 3rd Cockerill, T.F. Smith, *Clin Microbiol Rev.* **2006**, *19*, 165-256.
9 M. Johnson III, J. Fresco, *Chromosoma* **1999**, *108*, 181–189.
10 C. Escude , T. Garestier and C. Helene, *Proc. Natl. Acad. Sci. U. S. A.*, **1999**, *96* , 10603-10607
11 T. Antony, T. Thomas, L. H. Sigal, A. Shirahata, T. J. Thomas, *Biochemistry* **2001**, *40*, 9387–9395.
12 I. Ghosh, C. I. Stains, A. T. Ooib, D. J. Segal, *Mol. BioSyst.*, **2006**, *2*, 551-560
13 A. Patterson, F. Caprio, A. Vallée-Bélisle, D. Moscone, K. W. Plaxco, G. Palleschi, F. Ricci, *Anal. Chem*. **2010**, *82*, *21*, 9109-9115.
14 K.R. Fox, T. Brown, D.A. Rusling, Chapter 1: DNA Recognition by Parallel Triplex Formation, in DNA-targeting Molecules as Therapeutic Agents, 2018, 1-32.
15 M. D. F. Kamenetskii, S. M. Mirkin, *Annu. Rev. Biochem.* **1995**, *64*, 65–95.
16 E. N. Nikolova, E. Kim, A. A. Wise, P. J. O'Brien, I. Andricioaei, H. M. Al-Hashimi, *Nature* **2011**, *470*, 498–504.
17 S. Tyagi, F. R. Kramer, *Nat. Biotechnol.* **1996**, *14*, 303–308.
18 B. L. Renard, R. Lartia and U. Asseline, *Org. Biomol. Chem.*, **2008**, *6*, 4413–4425.
19 S. Ikeda, H. Yanagisawa, M. Yuki and A. Okamoto, *Artif. DNA PNA XNA,* **2013**, *4*, 19–27.
20 O. Doluca, T. K. Hale, P. J. B. Edwards, C. Gonzalez and V. V. Filichev, *ChemPlusChem,* **2014**, *79*, 58–66.
21 S. Walsh, A. H. El-Sagheer, T. Brown, *Chem. Sci.* **2018**, *9*, 7681–7687.
22 H. Asanuma, M. Akahane, N. Kondo, T. Osawa, T. Kato, H. Kashida, *Chem. Sci.* **2012**, *3*, 3165–3169.
23 H. Asanuma, M. Akahane, R. Niwa, H. Kashida, Y. Kamiya, *Angew. Chem. Int. Ed.* **2015**, *54*, 4315-4319.
24 H. Kashida, N. Kondo, K. Sekiguchi, H. Asanuma, *Chem. Commun.* **2011**, *47*, 6404-6406.
25 When two clear sigmoid transitions from melting of Hoogsteen base pairs and Watson-Crick base pairs were observed in the UV-melting curves, we calculated T_m values from these transitions. In other cases, T_m values of melting of the triplex could not be determined due to the overlap between two sigmoid curves, and we used fluorescence-melting for the calculation of the T_m.
26 C. Helsen, T. Van den Broeck, A. Voet, S. Prekovic, H.V. Poppel, S. Joniau, F. Claessens, *Endocr. Relat. Cancer* **2014**, *21*, T105–T118.
27 M. K. Graham, T. R. Brown, P. S. Miller, *Biochemistry* **2015**, *54*, 2270–2282.
28 H. Kashida, T. Takatsu, T. Fujii, K. Sekiguchi, X. Liang, K. Niwa, T. Takase, Y. Yoshida, H. Asanuma, *Angew. Chem., Int. Ed.,* **2009**, *48*, 7044-7047.
29 First, we synthesized TFO linear probes containing **Q** as we previously reported.[23] However, this modification destabilized the DNA triplex, and signal emission was significantly lower than that of the probe without **Q**, likely due to the strong interaction between anthraquinone and perylene in both single-stranded and triplex states (Fig. S7).

